

Teemu Hynninen, Hannes Raebiger, and Juhani von Boehm. 2006. A multiscale study of ferromagnetism in clustered (Ga,Mn)N. *Journal of Physics: Condensed Matter*, volume 18, pages 1561-1567.

© 2006 Institute of Physics Publishing

Reprinted with permission.

<http://www.iop.org/journals/jpcm>  
<http://stacks.iop.org/jpcm/18/1561>

## A multiscale study of ferromagnetism in clustered (Ga,Mn)N

Teemu Hynninen, Hannes Raebiger<sup>1</sup> and Juhani von Boehm

COMP/Laboratory of Physics, Helsinki University of Technology, 02015 HUT, Finland

E-mail: [hra@fyslab.hut.fi](mailto:hra@fyslab.hut.fi)

Received 8 November 2005

Published 17 January 2006

Online at [stacks.iop.org/JPhysCM/18/1561](http://stacks.iop.org/JPhysCM/18/1561)

### Abstract

Magnetic interactions in (Ga,Mn)N are studied on the microscopic inter-cluster and intra-cluster scales using first-principles calculations. Ferromagnetic transition temperatures are calculated using Monte Carlo methods. Randomness in Mn substitution is found to reduce Curie temperatures by about 10–20% from those of the corresponding regular (Ga,Mn)N lattice due to clustering. Nevertheless, high Curie temperatures reaching above room temperature are obtained even for completely random Mn distribution in (Ga,Mn)N for the Mn concentration of  $x \geq 13.5\%$ . Increasing clustering is always found to decrease the Curie temperature—especially when tetramer clusters are formed.

The active search for diluted magnetic semiconductors (DMSs) with high Curie temperatures ( $T_C$ s) exceeding room temperature started with the discovery of ferromagnetism in (In,Mn)As [1]. The calculations by Dietl *et al* predicted that (Ga,Mn)N should have the highest  $T_C$  ( $\simeq 400$  K) among the prospective III–V DMS materials suggested for spintronics applications [2]. However, the measured  $T_C$  values for (Ga,Mn)N range from 10 to 940 K [3–6] and also paramagnetic behaviour is reported at lower Mn concentrations (typically  $x < 0.02$ ) [7]. The reasons for the wide range of the observed  $T_C$  values and especially for the high values are poorly understood. One of the suggestions for this anomalous behaviour of  $T_C$  is that the increase is due to clustering (or precipitation) of Mn atoms and the formation of giant magnetic moments at the Mn clusters [6, 8–10]. However, Mn clustering is usually found to decrease calculated  $T_C$ s [11–15] although in some very special situations an increase may also be obtained [9–11].

In this paper we consider small clusters and define a  $Mn_n$  cluster as a collection of  $n$  substitutional Mn atoms ( $n = 2, 3$ , and 4 for dimers, trimers, and tetramers, respectively) which have a common N neighbour. At high Mn concentrations  $x$  a considerable amount of Mn clusters are present even in the case of a completely *random* distribution of substitutional

<sup>1</sup> Author to whom any correspondence should be addressed.

Mn atoms. For example, at  $x = 0.10$ , more than 60% of the Mn atoms belong to clusters [10]. Furthermore, cluster formation is energetically favourable [8, 10, 16], suggesting that even larger cluster portions may be expected. At these substitutional Mn clusters large stable magnetic moments are formed [8, 10, 16, 17]. Therefore, the interactions between the cluster spins (inter-cluster interactions) may be expected to actually determine the magnetic properties of the material instead of the interactions between the individual Mn atom spins.

In the present paper our aim is to consider both the microscopic structure and the microscopic cluster interactions in the calculations of  $T_C$  for (Ga,Mn)N because these interactions vary sensitively with respect to the cluster size [10, 16]. We will show that high  $T_C$  values reaching above room temperature can be achieved even for fully *random* Mn distribution in (Ga,Mn)N when  $x \geq 13.5\%$  and that randomness in Mn substitution reduces  $T_C$  unexpectedly little (*only* by about 10–20%) from the corresponding regular (Ga,Mn)N lattice. This is a direct consequence of the relatively long interaction ranges of our calculated exchange constants causing also low percolation thresholds. We also find that the formation of tetramer clusters reduces  $T_C$  strongly.

First, we perform density functional supercell calculations using the projector augmented wave method (VASP code) [18] to determine (i) cluster distributions at thermal equilibrium and (ii) magnetic interactions. We use the generalized gradient approximation (GGA-PW91) for exchange–correlation and the plane wave cut-off is 425 eV. The optimized wurtzite lattice parameters  $a = 3.217 \text{ \AA}$  and  $c:a = 1.631$  are used throughout in supercells of 48–108 atoms applying similar  $\vec{k}$ -meshes to those in [10]. We calculate similarly to [15] binding energy values which are used in Metropolis Monte Carlo (MC) simulations [19] for the determination of the structures (i). For the magnetic interactions (ii) we calculate total energies for the different spin alignments inside small clusters (Mn<sub>2</sub>–Mn<sub>4</sub>, intra-cluster energies) as well as for the different cluster spin alignments for the pairs of clusters (inter-cluster energies; also, Mn<sub>1</sub> monomers included) [10, 20]. The total intra-cluster and inter-cluster spin-flip energies are then mapped onto a modified classical Heisenberg Hamiltonian

$$H = - \sum_{(i,j)} J_{n_i n_j}(r_{ij}) \mathbf{s}_i \cdot \mathbf{s}_j - \sum_i E_{n_i}(s_i). \quad (1)$$

Here  $(i, j)$  denotes a sum over all pairs of clusters,  $n_i$  gives the type of cluster  $i$  ( $n_i = 1, 2, 3$ , and 4 for a monomer, dimer, trimer, and tetramer, respectively),  $r_{ij} = |\mathbf{r}_i - \mathbf{r}_j|$  is the distance between the centres of mass of the Mn clusters  $i$  and  $j$ , and the cluster spin  $\mathbf{s}_i$  is the effective classical spin vector of the Mn cluster  $i$ .  $\mathbf{s}_i$  is obtained as a mean vector sum of the  $n_i$  classical spin unit vectors  $\mathbf{e}_{ik}$  of the individual Mn atoms in the cluster as

$$\mathbf{s}_i = \sum_k \mathbf{e}_{ik} / n_i, \quad (2)$$

which makes  $s_i = |\mathbf{s}_i|$  vary between 0 and 1. We are forced to introduce the energy function  $E_{n_i}$  in equation (1) which gives the total internal energy of the cluster  $i$  because we find in agreement with reference [16] that *ab initio* intra-cluster spin-flip energies cannot be mapped onto a pairwise Heisenberg Hamiltonian. The  $E_{n_i}$  functions are constructed as follows. The values of  $E_{n_i}(s_i)$  for the collinear spin alignments are directly the *ab initio* intra-cluster energy values, while the non-collinear  $E_{n_i}$  values are interpolated. As a guideline we use the well known expression for the total energy of the Mn<sub>2</sub> dimer

$$E_2(s_i) = E' - J \mathbf{e}_{i1} \cdot \mathbf{e}_{i2} = E_2(1) + [E_2(0) - E_2(1)](1 - s_i^2), \quad (3)$$

where the dependence on  $s_i$  is quadratic. We use the same quadratic interpolation to obtain the non-collinear values in  $E_3$  and  $E_4$ .

The inter-cluster exchange coefficients  $J_{n_i n_j}$  are obtained by fitting  $H$  of equation (1) to the *ab initio* spin-flip energies. We first fit the  $J_{12}$  for the monomer–dimer pair for which

**Table 1.** Monomer–cluster binding energies. These binding energies are calculated using 72-atom supercells as described in [10].

	$\Delta E$ (meV)
$\text{Mn}_1 + \text{Mn}_1 \longleftrightarrow \text{Mn}_2$	521
$\text{Mn}_1 + \text{Mn}_2 \longleftrightarrow \text{Mn}_3$	615
$\text{Mn}_1 + \text{Mn}_3 \longleftrightarrow \text{Mn}_4$	622

we obtained a high spin-flip energy [10]. The fit is done on ten *ab initio* values calculated at different separations. After trying several decaying functions of the form of  $\exp(-\gamma r)$  or  $r^{-n}$  ( $n = 1, 2, 3,$  and  $4$ ) we found that  $r^{-3}$  most naturally describes the general behaviour. The best fit is then obtained by choosing a function composed of the decaying  $r^{-3}$  term and a local term describing a peak at 6 Å:

$$\frac{A}{r^3} + B(r - r_1)e^{-\alpha(r-r_2)^2}, \quad (4)$$

where  $A$ ,  $B$ ,  $r_1$ ,  $\alpha$ , and  $r_2$  are constants. We choose this same form for the other cluster pairs as well, and assume that the local term has the same shape, i.e.  $\alpha$ ,  $r_2 - r_1$ , and  $Br_1^3/A$  are kept the same for all cluster pairs. The remaining coefficients  $A$  and  $r_1$  are fitted independently for all other cluster pairs using 2–3 calculated *ab initio* values. In our supercells the cluster–cluster separation reaches up to 11 Å, but in the fitting we also include the coupling to periodic images up to the cut-off radius of 13 Å ( $\approx 4a$ ). This cut-off is also used throughout the MC simulations, i.e. the magnetic coupling beyond 13 Å equals zero. Directional dependences of the couplings are not explicitly included in expression (4), although they may be significant [21, 22]. Nevertheless, different directions and supercell shapes were included in the fitting of  $J_{12}$ , giving a rather good fit with expression (4), although this expression excludes directional effects. As the result of using expression (4) the spin-flip energies calculated with the Hamiltonian of equation (1) mostly differ by less than 3 meV from the corresponding *ab initio* values and even in the worst case this difference remains less than 9 meV.<sup>2</sup> Figure 1 shows the resulting ten  $J_{n_i n_j}$  exchange coefficients needed to describe the magnetic interactions.

We consider two different Mn cluster distributions: a fully random distribution and a distribution in thermal equilibrium at 1000 K. The former is obtained simply by randomly replacing Ga atoms by Mn atoms, and the latter is obtained from a Metropolis MC simulation [19] using the *ab initio* binding energies given in table 1. The cluster portions for these two distributions are given in figure 2 as a function of  $x$ . In the case of the random distribution (left wide columns) one immediately notices the relatively large dimer portion at large  $x$  while the trimer portion and especially the tetramer portion remain small. In the case of the thermal equilibrium distribution at 1000 K (right narrow columns) we see that considerable clustering has taken place: almost all monomers have vanished and the portion of dimers has considerably diminished, while the portion of the trimers and especially that of the tetramers have grown markedly. We also briefly glance at percolation threshold Mn concentrations at which a percolation network of cluster pairs with  $J_{n_i n_j} > 0$  meV is formed. We find for the random distribution and the thermal equilibrium distribution at 1000 K low percolation thresholds of  $x \approx 0.01$  and  $0.03$ , respectively.

To estimate Curie temperatures based on the classical Hamiltonian of equation (1) we carry out MC simulations in two alternating stages keeping the atomic configuration fixed. The Wolff

<sup>2</sup> For a more stringent test we calculated also spin-flip energies not used in fitting for two monomers separated by 5.25 Å and for two dimers separated by 8.5 Å. The Hamiltonian of equation (1) gives values that are lower than the *ab initio* values by 7 and 20 meV, respectively.

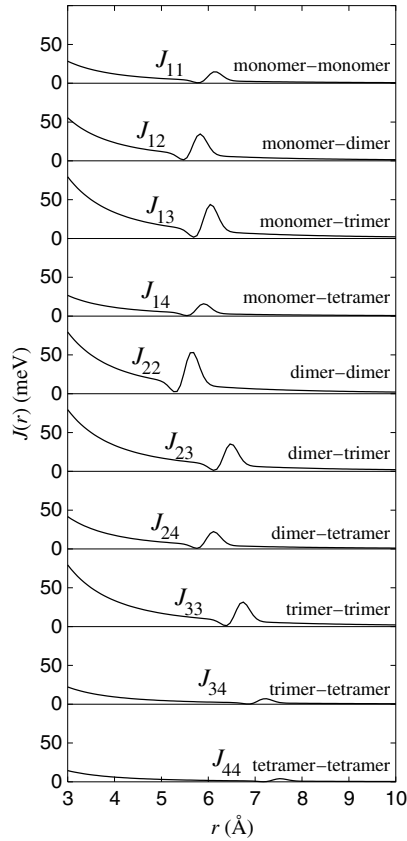


**Figure 1.** Inter-cluster exchange constants  $J_{n_i n_j}$ . The distance is measured between the centres of mass of the Mn atoms of the two clusters.

algorithm [23] is used to sample the classical cluster spins  $\mathbf{s}_i$  and the Metropolis algorithm [19] to sample the classical spin unit vectors  $\mathbf{e}_{ik}$  of the individual Mn atoms inside each cluster. Finite size effects are taken into account using Binder's cumulant method [24]. We generate Mn distributions having the same cluster portions as in figure 2 in the MC cells consisting of about 55 300–187 000 atoms. Each simulation is replicated 20–50 times which gives  $T_C$  with an accuracy of about 3 K.

Our calculated  $T_C$ s for the random distribution and the thermal equilibrium distribution at 1000 K are given in figure 3 (filled squares and circles, respectively).  $T_C$  depends on the Mn concentration  $x$  linearly. Our approach using ten slowly decaying  $J_{n_i n_j}$ s leads to higher  $T_C$ s than that using the more rapidly decaying exchange constant obtained from the coherent potential approximation (CPA) (compare filled squares with the open squares and circles from [25, 26] in figure 3). This difference may be attributed to different treatments of microscopic interactions in our and in the CPA calculations. We also calculated  $T_C$ s for regular monomer and monomer–dimer lattices. These values are around 10–20% higher than the  $T_C$ s for the random distribution (compare filled diamonds and triangle with the filled squares in figure 3).  $T_C$  for the random distribution is seen to exceed room temperature at the Mn concentration of about 13.5%. However, in thermal equilibrium at 1000 K, where significant clustering has taken place (compare the narrow right columns with the wide left ones in figure 2) we see a large drop in  $T_C$  which is directly related to clustering.

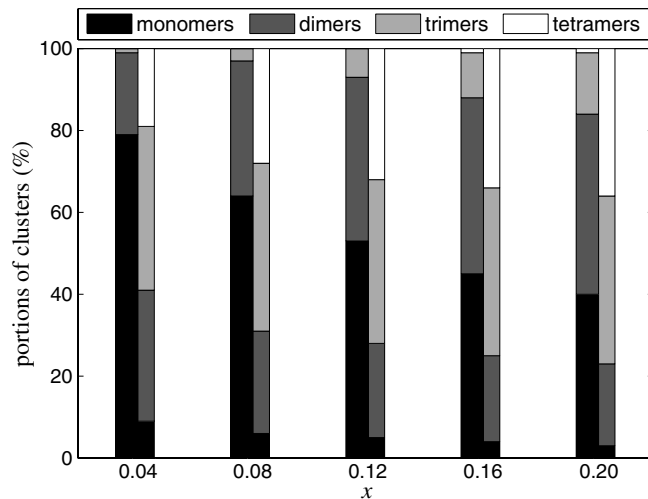


**Figure 2.** Percentage portions of clusters in the case of random distribution of substitutional Mn atoms (wide left columns) and in the case of thermal equilibrium at  $T = 1000$  K (narrow right columns).

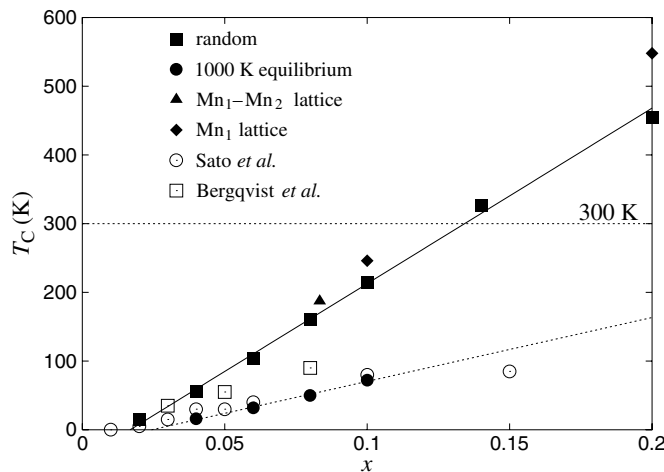


**Figure 3.** Calculated Curie temperatures  $T_C$  for the random substitutional Mn distribution (filled squares), the thermal equilibrium Mn distribution at 1000 K (filled circles), the regular monomer-dimer lattice (filled triangle), and the regular monomer lattice (filled diamonds). Also the CPA values calculated by Bergqvist *et al.* [25] (open squares) and Sato *et al.* [26] (open circles) are given for comparison. The lines are only to guide the eye.

Clustering reduces  $T_C$  for two principal reasons. First, clustering leads to an overall increase in inter-cluster separations and simultaneously decreases the number of clusters which apparently has a tendency to decrease  $T_C$ . Second, the microscopic inter-cluster exchange coefficients  $J_{n_i n_j}$  depend sensitively on the cluster size with a net effect of reducing  $T_C$ . This can be seen by comparing the  $J_{n_i n_j}$ s in figure 1. It is immediately clear that all  $J_{n_i 4}$ s with a tetramer as a partner are significantly weaker than the corresponding other  $J_{n_i n_j}$ s:  $J_{14}$  is weaker than  $J_{12}$  and  $J_{13}$ ;  $J_{24}$  is weaker than  $J_{22}$  and  $J_{23}$ ;  $J_{44}$  is weaker than  $J_{34}$  that is weaker

than  $J_{33}$ . Thus, when the portion of tetramers in thermal equilibrium at 1000 K grows up to 20–40% (depending on  $x$ ; figure 2) it is natural that the  $T_C$  values undergo the dramatic drop shown in figure 3 (compare the filled circles with the filled squares). We also calculated the thermal equilibrium distribution at 600 K for  $x = 0.1$  and found that the portion of tetramers was grown to 70% and that  $T_C$  attains an even lower value of only 21 K (not shown in figure 3). Finally, we note that the high mean-field value of 514 K obtained for the regular monomer–dimer lattice at  $x = 0.08$  [10] has lowered drastically to the value of 187 K (filled triangle in figure 3) which is due to the inclusion of magnetic fluctuations and intra-cluster energies  $E_{n_i}$  in the present calculations. A similar large drop in  $T_C$  for (Ga,Cr)N (from 600 to less than 50 K) is found in [12].

Our total spin-flip energies are obtained using the GGA which contains artificial self-interaction. We have studied its influence using the local density approximation (LDA) +  $U$  approach with  $U = 3$  eV. We found that the calculated spin-flip energies mostly increased by of the order of 10% [10] suggesting that a similar increase in  $T_C$  may be expected. Sandratskii *et al* using the LDA +  $U$  approach with  $U \approx 4$  eV find a strong increase from the LDA values:  $T_C$  grows from about 300 K to almost 700 K [27].

In conclusion, we find, using a combined *ab initio*–Monte Carlo method where the microscopic magnetic inter- and intra-cluster interactions are included, that high Curie temperatures reaching above room temperature can be achieved even for fully *random* Mn distribution in (Ga,Mn)N when the Mn concentration exceeds 13.5% and that in general randomness reduces the Curie temperatures by only about 10–20% from the corresponding Curie temperatures of regular (Ga,Mn)N lattices. We find a strong decrease in Curie temperatures when significant amounts of tetramer clusters are formed.

## Acknowledgments

This work was supported by the Academy of Finland through the Centre of Excellence Programme (2000–2005) and HR was supported by the Finnish Cultural Fund. The authors are grateful for the inspiring discussions with Professor K Saarinen before his too early passing away. The authors thank Acad. Professor R M Nieminen, Professor T Ala-Nissilä, and Drs M Alava, A Harju, and A Ayuela for many valuable discussions. The computing resources from the Centre for Scientific Computing (CSC) are acknowledged.

## References

- [1] Munekata H, Ohno H, von Molnar S, Armin Segmüller, Chang L L and Esaki L 1989 *Phys. Rev. Lett.* **63** 1849
- [2] Dietl T, Ohno H, Matsukura F, Cibert J and Ferrand D 2000 *Science* **287** 1019
- [3] Overberg M E, Abernathy C R, Pearton S J, Theodoropoulou N A, McCarthy K T and Hebard A F 2001 *Appl. Phys. Lett.* **79** 1312
- [4] Sasaki T, Sonoda S, Yamamoto Y, Suga K, Shimizu S, Kindo K and Hori H 2002 *J. Appl. Phys.* **91** 7911
- [5] Thaler G T, Overberg M E, Gila B, Frazier F, Abernathy C R, Pearton S J, Lee J S, Lee S Y, Park Y D, Khim Z G, Kim J and Ren F 2002 *Appl. Phys. Lett.* **80** 3964
- [6] Dhar S, Brandt O, Trampert A, Däweritz L, Friedland K J, Ploog K H, Keller J, Beschoten B and Güntherodt G 2003 *Appl. Phys. Lett.* **82** 2077
- [7] Giraud R, Kuroda S, Marcet S, Bellet-Amalric E, Biquard X, Barbara B, Fruchart D, Ferrand D, Gibert J and Mariette H 2004 *Europhys. Lett.* **65** 553
- [8] Rao B K and Jena P 2002 *Phys. Rev. Lett.* **89** 185504
- [9] Bouzzerar G, Ziman T and Kudrnovský J 2004 *Appl. Phys. Lett.* **85** 4941
- [10] Hynninen T, Raebiger H, Ayuela A and von Boehm J 2005 *Preprint cond-mat/0508522*
- [11] Sandratskii L M, Bruno P and Mirbt S 2005 *Phys. Rev. B* **71** 045210
- [12] Xu J L, van Schilfhaarde M and Samolyuk G D 2005 *Phys. Rev. Lett.* **94** 097201

- 
- [13] Sandratskii L M and Bruno P 2004 *J. Phys.: Condens. Matter* **16** L523
  - [14] Raebiger H, Ayuela A and Nieminen R M 2004 *J. Phys.: Condens. Matter* **16** L457
  - [15] Raebiger H, Ayuela A and von Boehm J 2005 *Phys. Rev. B* **72** 014465
  - [16] van Schilfgaarde M and Mryasov O N 2001 *Phys. Rev. B* **63** 233205
  - [17] Das G P, Rao B K and Jena P 2003 *Phys. Rev. B* **68** 035207
  - [18] Kresse G and Furthmüller J 1996 *Phys. Rev. B* **54** 11169  
Kresse G and Furthmüller J 1999 *VASP the Guide* (Vienna: Vienna University of Technology)  
<http://tph.tuwien.ac.at/~vasp/guide/vasp.html>
  - [19] Metropolis N, Rosenbluth A W, Rosenbluth M N, Teller A H and Teller E 1953 *J. Chem. Phys.* **21** 1087
  - [20] Hynninen T, Raebiger H, Ayuela A and von Boehm J 2006 unpublished
  - [21] Kudrnovský J, Turek I, Drchal V, Mácá F, Weinberger P and Bruno P 2004 *Phys. Rev. B* **69** 115208
  - [22] Mahadevan P, Zunger A and Sarma D D 2004 *Phys. Rev. Lett.* **93** 177201
  - [23] Wolff U 1989 *Phys. Rev. Lett.* **62** 361
  - [24] Binder K 1981 *Phys. Rev. Lett.* **47** 693
  - [25] Bergqvist L, Eriksson O, Kudrnovský J, Drchal V, Korzhavyi P and Turek I 2004 *Phys. Rev. Lett.* **93** 137202
  - [26] Sato K, Schweika W, Dederichs P H and Katayama-Yoshida H 2004 *Phys. Rev. B* **70** 201202(R)
  - [27] Sandratskii L M, Bruno P and Kudrnovský J 2004 *Phys. Rev. B* **69** 195203